

Supplementary Materials

A. Experimental Details

Table 1. Dataset details

	CT-MRI	FLAIR-T1
#total	219	1470
#train	197	1251
#test	22	219
shape	160×160×160	176×176×160
voxel size	1×1×1mm ³	

Table 2. Implementation details

	CT→MRI	FLAIR→T1
batch size	16	8
#iterations	100,000	150,000
λ	0.5	0.05
time step	1000	
sampling step	100	
GPU	NVIDIA RTX A6000	

B. Additional Qualitative Comparison

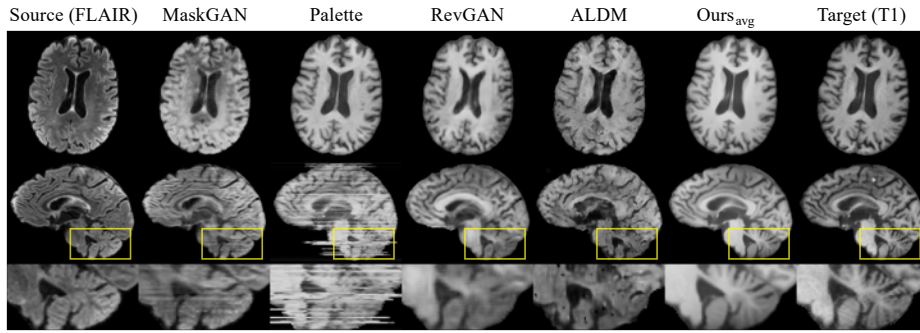


Fig. 1. Qualitative comparison with baselines (FLAIR→T1)

C. Derivation of Score Function $S_\theta(\mathbf{X}_t, \mathbf{c}_{SKC}, t)$ for θ Trained as $\theta = \theta^*$

Since $\mathbf{E}_{\theta^*, t} = CP_{\theta^*}(\mathbf{X}_t, \mathbf{c}_{SKC}, t) = m_t(\mathbf{Y} - \mathbf{X}_0) + \sqrt{\delta_t}\boldsymbol{\epsilon}_t$, where $\boldsymbol{\epsilon}_t \in \mathbb{R}^{Z \times H \times W}$,

$$CP_{\theta^*}(\mathbf{X}_t, \mathbf{c}_{SKC}, t) = \mathbf{X}_t - \mathbf{X}_0 \quad (\because \mathbf{X}_t = (1 - m_t)\mathbf{X}_0 + m_t\mathbf{Y} + \sqrt{\delta_t}\boldsymbol{\epsilon}_t).$$

$$\text{Then, } CP_{\theta^*}(\mathbf{X}_t, \mathbf{c}_{SKC}, t) = m_t[\mathbf{Y} - \{\mathbf{X}_t - CP_{\theta^*}(\mathbf{X}_t, \mathbf{c}_{SKC}, t)\}] + \sqrt{\delta_t}\boldsymbol{\epsilon}_t$$

$$\iff \boldsymbol{\epsilon}_t = \frac{1}{\sqrt{\delta_t}}\{m_t(\mathbf{X}_t - \mathbf{Y}) + (1 - m_t)CP_{\theta^*}(\mathbf{X}_t, \mathbf{c}_{SKC}, t)\}.$$

Thus, $S_{\theta^*}(\mathbf{X}_t, \mathbf{c}_{SKC}, t) = \nabla_{\mathbf{X}_t} \log q_{BB}(\mathbf{X}_t | (1 - m_t)\mathbf{X}_0 + m_t\mathbf{Y}, \mathbf{c}_{SKC})$

$$= -\frac{[\mathbf{X}_t - \{(1 - m_t)\mathbf{X}_0 + m_t\mathbf{Y}\}]}{\delta_t} = -\frac{\boldsymbol{\epsilon}_t}{\sqrt{\delta_t}} \quad (\text{cf. } \nabla_{\tilde{\mathbf{x}}} \log q_\sigma(\tilde{\mathbf{x}} | \mathbf{x}) = -\frac{\tilde{\mathbf{x}} - \mathbf{x}}{\sigma^2} \text{ in [1]}),$$

since \mathbf{X}_t is the Gaussian perturbation of $(1 - m_t)\mathbf{X}_0 + m_t\mathbf{Y}$.

$$\therefore S_{\theta^*}(\mathbf{X}_t, \mathbf{c}_{SKC}, t) = -\frac{1}{\delta_t}\{m_t(\mathbf{X}_t - \mathbf{Y}) + (1 - m_t)CP_{\theta^*}(\mathbf{X}_t, \mathbf{c}_{SKC}, t)\}.$$

D. Qualitative Results of Ablation Study

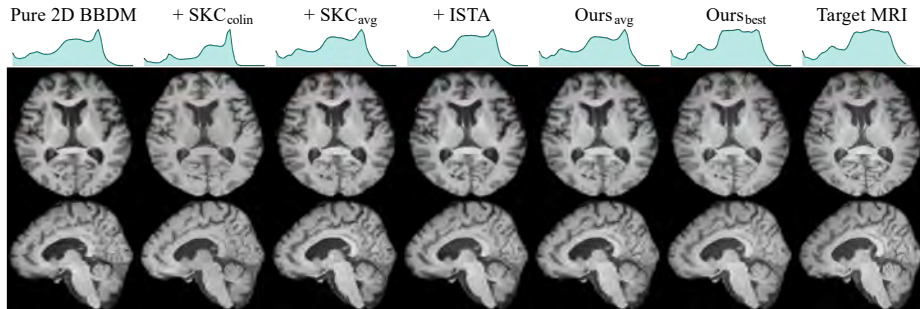


Fig. 2. Qualitative comparison with baselines (CT→MRI)

E. Additional Study for Style Key Conditioning

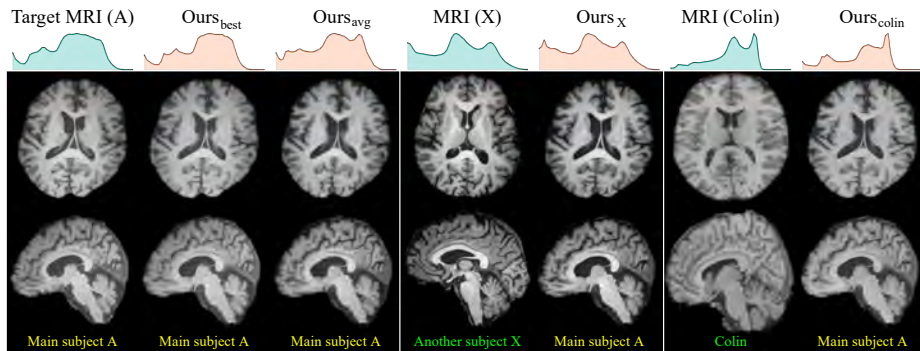


Fig. 3. Qualitative results for various style keys (CT→MRI). Figure shows real MRIs of main subject A, another subject X, and Colin 27 Average Brain (public access), along with synthetic MRIs of subject A. Both $Ours_x$ and $Ours_{colin}$ present synthetic MRIs of subject A, each transformed into the respective styles of X and Colin. From the analysis of the intensity histogram presented above, we observe that $Ours_x$ closely matches the MRI histogram of subject X, while $Ours_{colin}$ aligns with that of Colin. This demonstrates that the style of MRIs can be effectively controlled using SKC.

References

1. Song, Y., Ermon, S.: Generative modeling by estimating gradients of the data distribution. *Advances in neural information processing systems* **32** (2019)